Global Features of the Semiannual Oscillation in Stratospheric Temperatures and Comparison between Seasons and Hemispheres

XIN-HAI GAO, WEN-BI YU* AND JOHN L. STANFORD

Department of Physics, Iowa State University, Ames, IA 50011

(Manuscript received 9 May 1986, in final form 13 October 1986)

ABSTRACT

Four years of satellite-derived microwave and infrared radiances are analyzed for the three-dimensional and seasonal variation of semiannual oscillations (SAO) in stratospheric temperatures, with particular focus on high latitudes, to investigate the effect of stratospheric warmings on SAO. Separate analyses of individual seasons in each hemisphere reveal that the strongest SAO in temperature occur in the Northern Hemisphere (NH) winter polar upper stratosphere. These results, together with the latitudinal structure of the temperature SAO and the fact that the NH polar SAO is nearly out of phase with the lower latitude SAO, are consistent with the existence of a global-scale, meridional circulation on the SAO time scale. The results suggest that polar stratospheric warmings are an important source of SAO in both high and low latitude stratospheric temperature fields. Interannual variations, three-dimensional phase structure, and zonal asymmetry of SAO are also detailed. The SH stratospheric SAO is dominated by a localized feature in the high-latitude, eastern hemisphere which tilts westward with height.

1. Introduction

The semiannual oscillation (SAO) of the zonal wind and zonal mean temperature in the tropical middle atmosphere has been studied by many investigators, beginning with the pioneering work of Reed (1962) who analyzed radiosonde temperature data and rocket wind measurements. He found maximum SAO amplitude at the equator in both temperature and mean zonal wind, characterized by downward phase propagation. Following Reed's work, many studies on mean zonal wind and temperature SAO have appeared (for example, Angell and Korshover, 1970; van Loon et al., 1972; McGregor and Chapman, 1978; Meyer, 1970; Takahashi, 1984). The structure and behavior of the tropical middle atmosphere SAO have been reviewed by Hirota (1980). In high latitudes, mean zonal wind and temperature SAO have been found by using rocket network and satellite data (Angell and Korshover, 1970; van Loon et al., 1972; Fritz, 1974; Nastrom and Belmont, 1975; Crane, 1979). Hamilton (1987) has recently investigated the contribution of eddies to the equatorial SAO, while Hitchman and Leovy (1986) have provided a detailed study of the evolution of the equatorial middle atmosphere, including the SAO, from analyses of LIMS data. Both of these papers also provide good reviews.

Calculations of solar-induced radiance (Fritz, 1974) suggested that solar radiation associated with the twice-yearly passage of the sun across the equator could not fully account for SAO at the equator, especially during the NH winter season. Fritz noted that tropical cooling during winter polar warmings might partly account for the tropical temperature SAO. However, few observational studies have been done to check this idea.

Compared with the tropics, less is known about the high latitude SAO. Its cause has been attributed to semiannual radiative heating variations caused by the cutoff in solar heating which occurs in the polar night (Holton and Wehrbein, 1980). Another possibility, mentioned briefly by Hirota (1980), is that high latitude SAO may be a consequence of midwinter polar vortex breakdown associated with stratospheric sudden warmings.

Hitchman and Leovy (1987), in analyses of LIMS data, found that the altitude of the high latitude stratopause exhibited a series of short-lived fluctuation events during the 1978/79 NH winter. Hitchman and Leovy suggested that the accumulation of such events, superimposed on the smoother annual cycle, leads to a semiannual component of the variation, at least in the north. Because the LIMS instrument measurements covered less than a year (October 1978–May 1979), they were only able to observe one NH winter; furthermore, it was not possible to harmonically analyze the data for SAO amplitudes.

In the present analysis, we utilize four-year time records of satellite microwave and infrared radiance measurements to obtain global distributions of SAO amplitude and phase for four atmospheric layers spanning the stratosphere. A quantitative estimate is given

* Permanent affiliation: Physics Department, Lanzhou University, Lanzhou, Gansu, People's Republic of China.

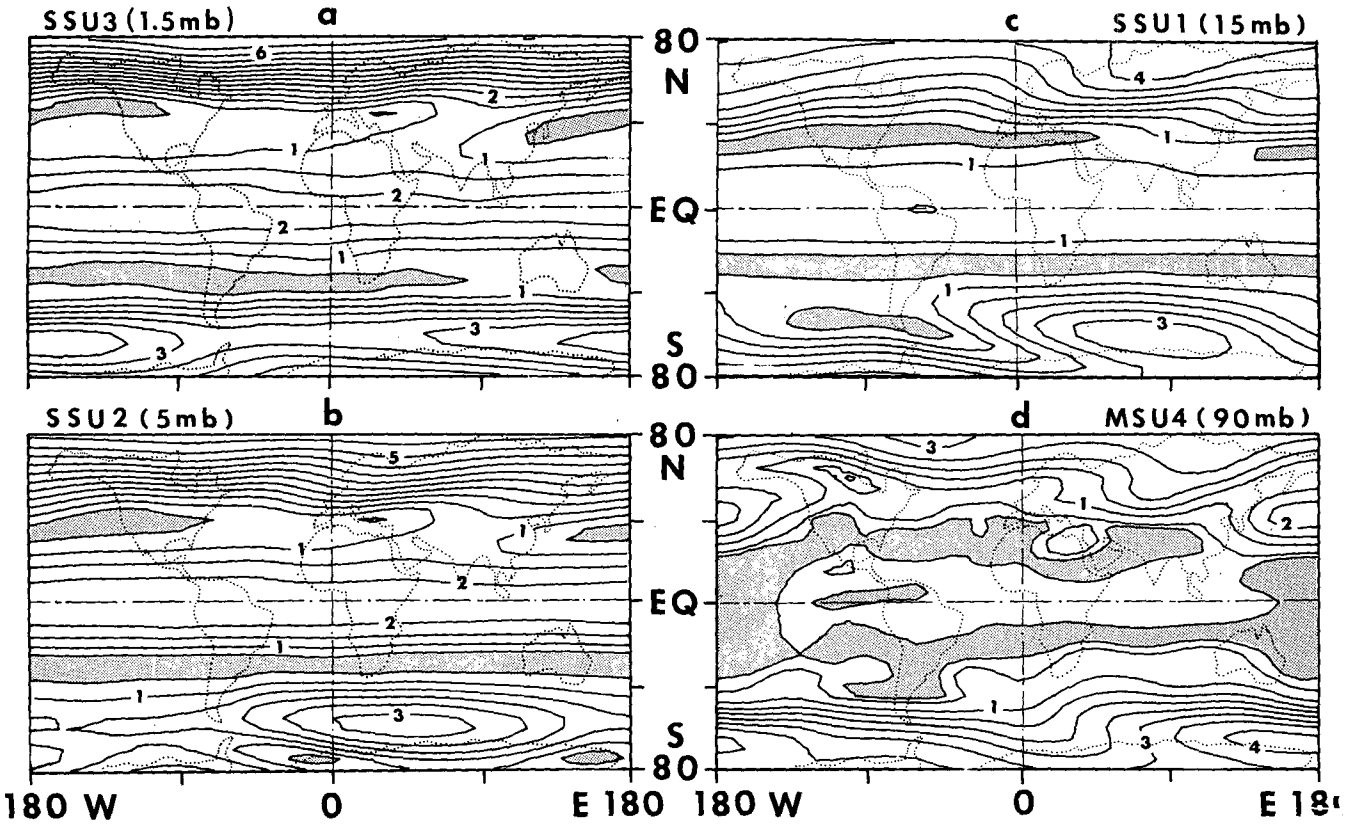

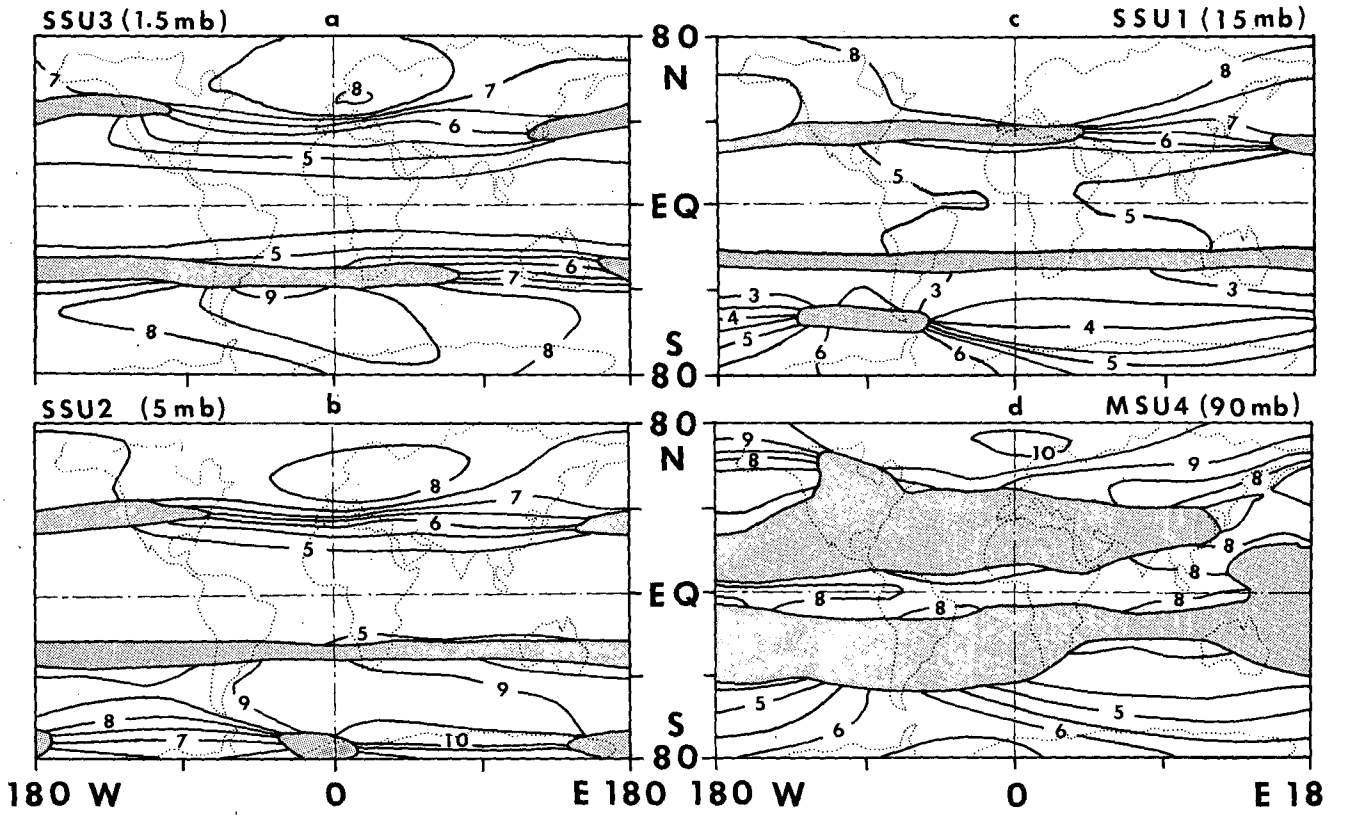

FIG. 2. As in Fig. 1 but of the phases. The numbers on the contours indicate one of the dates when the SAO reaches its maximum. For example, number 1 indicates January 2, 10 indicates October 2. The phase contour interval is one half month. Small amplitude regions are shaded.

TABLE 1. Phase (month/day of maximum) of SAO in zonal mean temperatures.

	Latitude (°S)					Latitude (°N)			
Channel	80	60	40	20	0	20	40	60	80
SSU3 (1.5 mb)	7/22	2/10	1/28	4/21	4/9	4/21	6/2	7/14	7/13
SSU2 (5 mb)	6/3	3/3	2/27	4/26	4/20	4/27	6/27	7/25	7/23
SSU1 (15 mb)	5/24	4/8	3/3	5/2	5/1	5/2	7/12	8/3	8/8
MSU4 (90 mb)	6/10	5/9	4/4	5/6	7/28	7/15	7/26	9/1	9/23

for the degree of departure from zonal symmetry in SAO, as well as seasonal and interannual variability. Particular attention is focused on the high latitudes in an attempt to investigate the effect of stratospheric warmings on the SAO in these regions. The results suggest that polar stratospheric warmings are an important source of SAO in both high and low latitude stratospheric temperature fields.

2. Data and analysis

The data used in this study are radiance measurements from NOAA satellites for MSU4 (Microwave Sounding Unit Channel 4) and three SSU (Stratospheric Sounding Unit) channels. The weighting functions of MSU4, SSU1, SSU2 and SSU3 peak near 90, 15, 5 and 1.5 mb, respectively. The daily 5° × 5° global grids were produced by the British Meteorological Office. The brightness temperatures (T_b) are calculated from radiance measurements by using the inverse Planck equation. The T_b are actually vertically-weighted mean temperatures, weighted by the instrumental weighting functions mentioned above. The SSU channels lie entirely within the stratosphere; the MSU4 channel is the mean 30–150 mb temperature, so that its measurements partly overlap the upper troposphere in the tropics where the high tropical tropopause usually is near 100 mb; outside the tropics, MSU4 data are representative of the lower stratosphere.

The brightness temperatures were analyzed for the period 1 April 1980 to 31 March 1984. Non-overlapping three day means were used to save computing time and memory. The effect on the SAO due to this processing is negligible. Spatial filtering using only zonal wavenumbers ≤ 10 was employed to suppress an instrumental "scan angle effect" (Yu and Stanford, 1984) as well as disturbances of small zonal scale, both of which represent unwanted noise in the present analyses. Details of the data processing are given in Gao and Stanford (1987).

The space and time Fourier coefficients are obtained by Fast Fourier Transformation. The space–time powers are calculated by the method reviewed in Hayashi (1982).

After removing spectral components with periods greater than six months, the four-year time series were divided into four winters (October through March) and

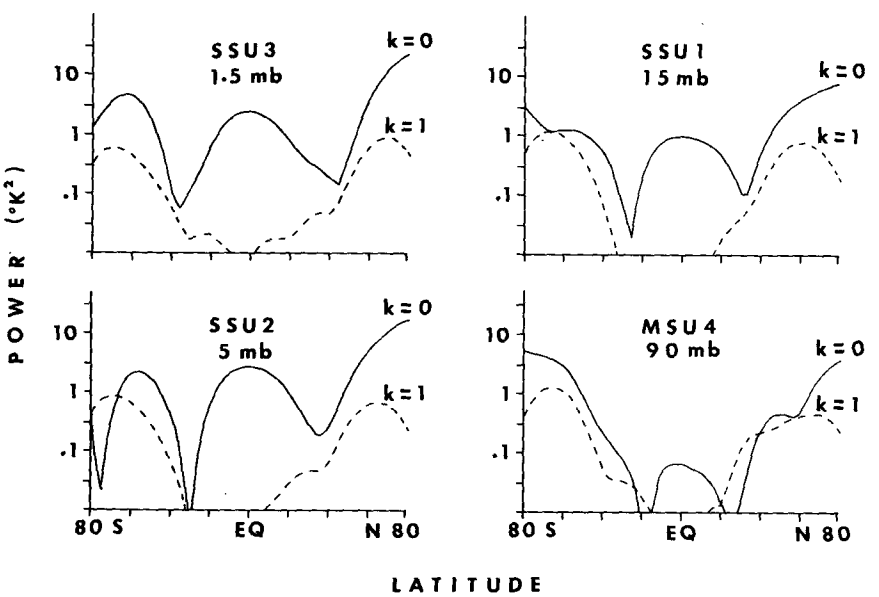

FIG. 3. Semiannual oscillation (SAO) power (°K²) for zonal wavenumber zero (solid lines) and zonal wavenumber one (dashed lines) as a function of latitude, plotted semilogarithmically. SSU3, 2, 1 and MSU4 represent layer temperatures centered near 1.5, 5, 15 and 90 mb, respectively.

TABLE 2a. Power (K^2) and phase (month/day of maximum) of SAO in zonal mean temperature for SSU3 (1.5 mb). Negative latitudes refer to the Southern Hemisphere.

Latitude (deg)	Apr 80 to Sep 80	Oct 80 to Mar 81	Apr 81 to Sep 81	Oct 81 to Mar 82	Apr 82 to Sep 82	Oct 82 to Mar 83	Apr 83 to Sep 83	Oct 83 to Mar 84
80	13.95	47.42	5.55	17.84	17.33	35.20	18.68	30.85
60	1.98	11.03	0.51	6.56	1.14	4.59	1.83	5.94
40	0.14	0.37	0.49	0.26	0.65	0.08	0.22	0.33
20	0.57	1.07	0.45	1.08	0.65	0.58	1.10	1.08
0	1.54	3.98	0.96	3.26	1.79	3.01	2.45	3.72
−20	0.18	1.01	0.21	1.22	0.45	0.80	0.40	0.86
−40	0.00	0.07	1.06	0.06	1.48	0.31	0.90	0.63
−60	3.78	4.38	9.81	6.24	8.25	5.36	4.06	3.11
−80	4.56	1.23	0.01	2.68	0.54	5.40	1.46	2.70
80	1/14	1/11	1/12	1/15	1/21	1/16	1/12	1/14
60	1/18	1/11	1/7	1/15	1/16	1/20	1/20	1/17
40	5/5	6/26	5/26	6/25	5/14	6/23	5/23	6/8
20	4/17	4/18	4/29	4/21	4/20	4/29	4/27	4/20
0	4/5	4/9	4/14	4/10	4/12	4/15	4/13	4/10
−20	4/23	4/20	5/8	4/22	4/21	4/23	4/25	4/21
−40	1/15	5/22	2/28	1/23	1/26	6/12	2/28	6/27
−60	3/4	2/11	2/24	2/7	2/8	1/28	2/17	1/22
−80	6/23	2/17	2/28	2/5	2/22	2/1	1/6	2/3

four summers (April through September). The time- and space-Fourier analyses were made separately for each winter and summer season, to facilitate study of the interannual and seasonal variability of the SAO.

3. Results and discussion

a. Global distribution of SAO amplitude

Figure 1 shows the global distribution of SAO amplitude for four layers spanning the stratosphere. Belts of maxima occur in the high latitudes of both hemispheres, as well as in the tropics. The low latitude SAO temperature amplitude increases with height, from 0.4 K in the lower to 2.4 K in the upper stratosphere, in agreement with Barnett's (1974) single year analysis of Nimbus 4 data. SAO amplitudes are twice as large in Northern as in Southern high latitudes, consistent with zonal mean magnitudes found for earlier years by van Loon et al. (1972). Note the strong SH feature south of Australia which appears to tilt westward with height.

b. Phase distributions

The phase distributions are given in Fig. 2. In the upper stratosphere, the SAO in high latitudes is nearly out of phase with that in the tropics, as seen in Fig. 2 and also in Table 1. In the vicinity of the SH strong amplitude feature, near 60°S in Fig. 1, the phase of

TABLE 2b. As in Table 2a but for SSU2 (5 mb).

Latitude (deg)	Apr 80 to Sep 80	Oct 80 to Mar 81	Apr 81 to Sep 81	Oct 81 to Mar 82	Apr 82 to Sep 82	Oct 82 to Mar 83	Apr 83 to Sep 83	Oct 83 to Mar 84
80	13.70	30.75	7.53	16.93	10.35	25.10	13.94	15.42
60	2.85	9.72	1.43	8.70	2.07	7.3	1.95	5.45
40	0.02	0.58	0.16	0.79	0.43	1.00	0.15	0.56
20	0.68	1.23	0.41	1.35	0.74	1.12	1.92	1.19
0	1.44	3.32	0.95	3.87	1.80	3.25	4.50	3.79
−20	0.13	0.75	0.17	1.15	0.38	0.90	0.88	0.58
−40	0.39	0.05	2.20	0.38	1.36	0.10	2.91	0.57
−60	2.88	1.90	7.96	2.93	3.32	1.51	3.27	0.78
−80	6.92	0.78	1.57	0.08	2.24	0.67	1.83	0.02
80	1/23	1/25	1/21	1/21	2/3	1/30	1/19	1/28
60	1/25	1/27	1/22	1/27	1/26	1/28	1/24	2/1
40	5/15	1/8	6/20	1/24	6/13	1/1	5/11	1/5
20	4/19	4/26	5/8	4/28	4/29	5/10	4/26	4/25
0	4/15	4/21	4/29	4/22	4/26	4/29	4/21	4/16
−20	4/20	4/28	5/17	4/28	4/30	5/3	4/20	4/19
−40	3/16	2/25	3/10	2/16	2/17	1/4	3/12	1/20
−60	4/1	2/28	3/16	2/24	2/27	2/14	3/11	1/28
−80	6/15	4/17	5/22	5/19	6/4	3/9	6/20	2/2

TABLE 2c. As in Table 2a but for SSU1 (15 mb).

Latitude (deg)	Apr 80 to Sep 80	Oct 80 to Mar 81	Apr 81 to Sep 81	Oct 81 to Mar 82	Apr 82 to Sep 82	Oct 82 to Mar 83	Apr 83 to Sep 83	Oct 83 to Mar 84
80	9.10	17.12	6.75	8.38	4.30	12.34	8.07	6.71
60	2.75	6.91	2.25	6.92	1.90	5.32	3.02	2.91
40	0.09	0.84	0.06	1.02	0.48	0.93	0.15	0.68
20	0.33	0.75	0.20	0.87	0.41	0.76	0.61	0.48
0	0.48	1.27	0.49	2.11	0.88	1.41	1.03	1.14
−20	0.02	0.35	0.06	0.61	0.13	0.39	0.16	0.18
−40	0.66	0.24	1.91	0.63	0.94	0.18	1.94	0.44
−60	2.88	2.04	5.40	1.11	0.80	0.63	1.30	0.08
−80	8.15	4.38	3.87	4.12	8.16	3.57	4.71	2.71
80	2/5	2/14	1/28	1/23	2/27	2/19	1/29	2/27
60	1/30	2/12	1/27	2/5	2/2	2/8	1/26	2/12
40	1/16	1/11	6/30	2/3	1/4	1/10	1/7	1/12
20	4/25	5/6	5/12	5/3	5/5	5/10	4/30	5/4
0	4/27	5/5	5/15	5/2	5/2	5/4	5/1	4/27
−20	4/18	5/10	5/23	5/3	4/30	5/6	4/23	4/27
−40	3/22	2/28	3/17	2/22	3/3	2/23	3/12	2/1
−60	4/30	4/10	4/8	3/25	4/3	3/29	4/5	4/30
−80	6/12	5/11	5/22	5/20	6/4	4/18	6/17	5/14

the 1.5 mb channel SAO signal precedes that at 15 mb by approximately 2 months.

c. *Southern Hemisphere SAO anomaly*

The Southern Hemisphere SAO amplitude distribution is dominated by the strong, localized SAO feature observed in the high latitudes of the Eastern Hemisphere. At least through the middle stratosphere the anomaly tilts westward with height. In the upper stratosphere it changes longitude so rapidly (nearly 180 deg between 5 and 1.5 mb) that it is difficult to tell from these layer-mean results whether it continues to tilt westward with height or changes to an eastward tilt. As noted above, Fig. 2 reveals clear downward phase velocity in the temperature SAO over the strong signal area. This suggests possible upward energy transport (group velocity) and heat flux associated with the anomaly, and warrants further investigation. To our knowledge this feature has neither been previously reported nor explained (although preliminary SH stratospheric zonal mean data presented by van Loon et al., 1972, Fig. 6, show its effect).

d. *SAO zonal asymmetry*

In addition to the SH anomaly in zonal symmetry, Fig. 1 reveals significant zonal asymmetry in the high latitudes of both hemispheres. Further details of the asymmetry are presented in Fig. 3 where the SAO power for zonal waves 0 (zonal mean) and 1 is plotted as a function of latitude for four layers spanning the

TABLE 2d. As in Table 2a but for MSU4 (90 mb).

Latitude (deg)	Apr 80 to Sep 80	Oct 80 to Mar 81	Apr 81 to Sep 81	Oct 81 to Mar 82	Apr 82 to Sep 82	Oct 82 to Mar 83	Apr 83 to Sep 83	Oct 83 to Mar 84
80	3.81	15.76	1.99	0.75	8.75	8.32	2.67	12.90
60	0.30	2.29	0.54	0.99	0.14	0.51	0.20	0.43
40	0.08	0.54	0.00	0.46	0.32	0.42	0.14	0.36
20	0.01	0.16	0.01	0.01	0.02	0.07	0.02	0.11
0	0.08	0.10	0.15	0.00	0.10	0.05	0.05	0.19
−20	0.03	0.01	0.00	0.05	0.03	0.05	0.02	0.01
−40	0.49	0.21	0.59	0.26	0.27	0.11	0.40	0.01
−60	4.04	4.12	4.29	2.65	2.49	2.94	2.42	2.13
−80	3.25	10.93	2.15	8.14	6.83	3.22	5.44	8.48
80	3/10	3/19	2/12	6/21	4/9	4/3	3/17	4/6
60	3/1	3/12	2/17	5/9	2/28	3/2	2/20	3/24
40	2/5	1/18	2/14	5/17	1/23	1/27	1/24	6/11
20	3/1	6/29	2/16	6/2	2/9	1/6	3/17	1/19
0	2/5	1/15	1/29	1/16	2/4	1/19	2/20	2/2
−20	4/8	5/29	1/9	5/4	3/24	6/25	5/2	6/20
−40	4/17	4/8	4/11	3/20	4/7	3/23	4/6	1/19
−60	5/19	5/8	5/9	5/6	5/15	5/7	5/13	5/12
−80	6/19	6/9	6/8	6/7	6/18	5/27	6/25	6/6

TABLE 3a. Power (K^2) of SAO in zonal wavenumber one for SSU3 and SSU2. Negative latitudes refer to the Southern Hemisphere.

Latitude (deg)	Apr 80 to Sep 80	Oct 80 to Mar 81	Apr 81 to Sep 81	Oct 81 to Mar 82	Apr 82 to Sep 82	Oct 82 to Mar 83	Apr 83 to Sep 83	Oct 83 to Mar 84
				SSU3				
80	0.48	0.18	0.08	0.12	0.20	0.11	0.57	0.06
60	0.47	0.02	0.10	0.18	0.43	0.13	0.69	0.03
40	0.09	0.05	0.05	0.04	0.22	0.04	0.27	0.10
20	0.03	0.07	0.01	0.04	0.03	0.03	0.04	0.01
0	0.01	0.03	0.01	0.02	0.00	0.02	0.01	0.01
−20	0.05	0.04	0.04	0.05	0.05	0.04	0.05	0.01
−40	0.36	0.13	0.22	0.10	0.12	0.06	0.20	0.02
−60	0.08	0.45	0.10	0.56	0.12	0.23	0.05	0.07
−80	0.14	0.25	0.36	0.29	0.10	0.16	0.22	0.03
				SSU2				
80	0.53	0.20	0.22	0.10	0.13	0.06	0.43	0.09
60	0.78	0.63	0.17	0.06	0.33	0.05	0.60	0.17
40	0.09	0.14	0.08	0.07	0.14	0.15	0.27	0.18
20	0.03	0.07	0.02	0.06	0.02	0.05	0.03	0.03
0	0.01	0.01	0.01	0.01	0.01	0.01	0.01	0.00
−20	0.03	0.02	0.01	0.03	0.04	0.02	0.01	0.00
−40	0.04	0.05	0.08	0.11	0.23	0.03	0.14	0.02
−60	0.19	0.11	0.17	0.29	0.05	0.24	0.22	0.01
−80	0.17	0.20	0.29	0.49	0.07	0.22	0.26	0.12

stratosphere. Channels SSU 1–3 lie entirely within the stratosphere in the tropics and show little zonal asymmetry. However, at high latitudes significant SAO wave 1 is found: at 15 mb over Antarctica, wave 1 is as strong as the zonal mean. Note that while the zonal mean SAO power is much greater in Northern Hemisphere high latitudes than in the Southern Hemisphere (except in the lower stratosphere), wave 1 has similar power in both high latitude regions.

Quantitative estimates of the asymmetry for all four layers as a function of latitude can be made by comparing the zonal mean results in Tables 2a–d with those for wave 1 in Tables 3a–b.

e. Interannual variations in SAO

Tables 2 and 3 also provide a measure of the interannual variability in SAO. The significant year-to-year variations are a clear indication that, besides solar heating (which presumably has no appreciable interannual variation over the four years studied), there must be other important sources for SAO in temperature.

TABLE 3b. As in Table 3a but for SSU1 and MSU4.

Latitude (deg)	Apr 80 to Sep 80	Oct 80 to Mar 81	Apr 81 to Sep 81	Oct 81 to Mar 82	Apr 82 to Sep 82	Oct 82 to Mar 83	Apr 83 to Sep 83	Oct 83 to Mar 84
				SSU1				
80	0.36	0.28	0.19	0.07	0.22	0.27	0.25	0.06
60	0.71	0.02	0.43	0.11	0.31	0.02	0.81	0.23
40	0.13	0.29	0.11	0.23	0.08	0.35	0.15	0.04
20	0.01	0.03	0.01	0.05	0.01	0.02	0.02	0.02
0	0.01	0.00	0.00	0.00	0.01	0.00	0.00	0.00
−20	0.02	0.00	0.01	0.01	0.01	0.00	0.00	0.00
−40	0.14	0.05	0.17	0.10	0.16	0.06	0.07	0.02
−60	0.28	0.35	0.52	0.50	0.40	0.42	0.15	0.08
−80	0.35	0.21	0.20	0.51	0.35	0.16	0.12	0.21
				MSU4				
80	0.28	0.16	0.28	0.04	0.49	0.08	0.20	0.07
60	0.47	0.05	0.78	0.08	0.20	0.05	0.79	0.04
40	0.32	0.41	0.26	0.17	0.12	0.14	0.34	0.19
20	0.01	0.04	0.03	0.01	0.03	0.02	0.03	0.01
0	0.00	0.01	0.01	0.00	0.00	0.00	0.01	0.00
−20	0.02	0.03	0.01	0.03	0.02	0.03	0.01	0.03
−40	0.16	0.20	0.17	0.17	0.14	0.18	0.10	0.05
−60	0.08	0.43	0.22	0.36	0.03	0.30	0.04	0.20
−80	0.13	0.39	0.16	0.61	0.59	0.19	0.34	0.29

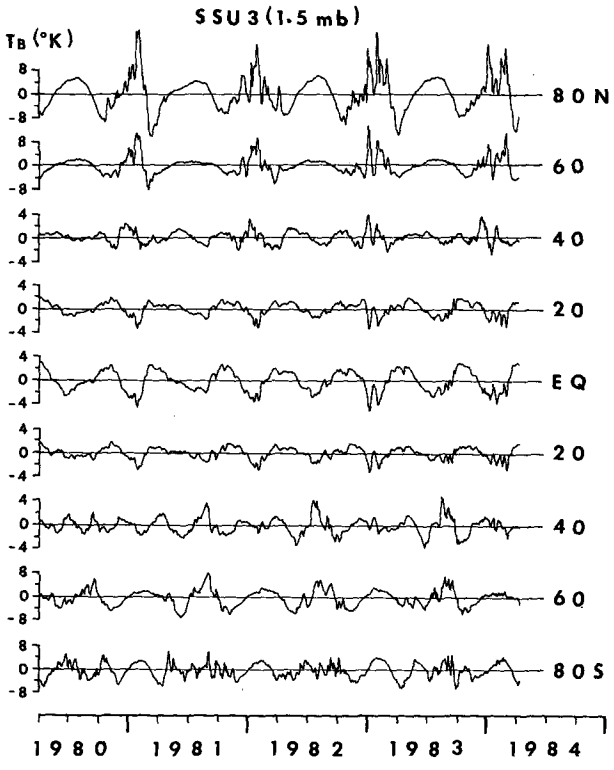

FIG. 4a. Zonal mean temperature (K) for SSU3 (1.5 mb) for 80°N–80°S and from 1 Apr 1980 to 31 Mar 1984. Harmonics whose periods are greater than six months have been removed. Note the change of scale at high latitudes.

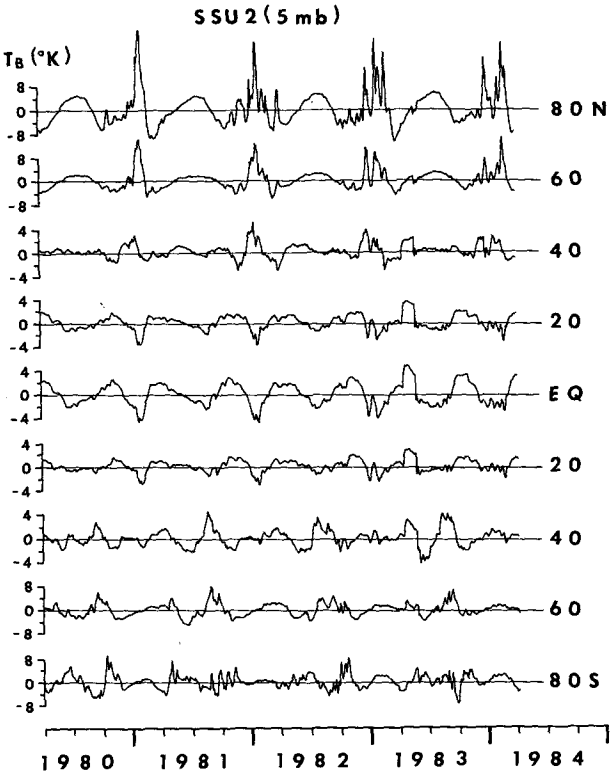

FIG. 4b. As in Fig. 4a but for (a) SSU2 (5 mb).

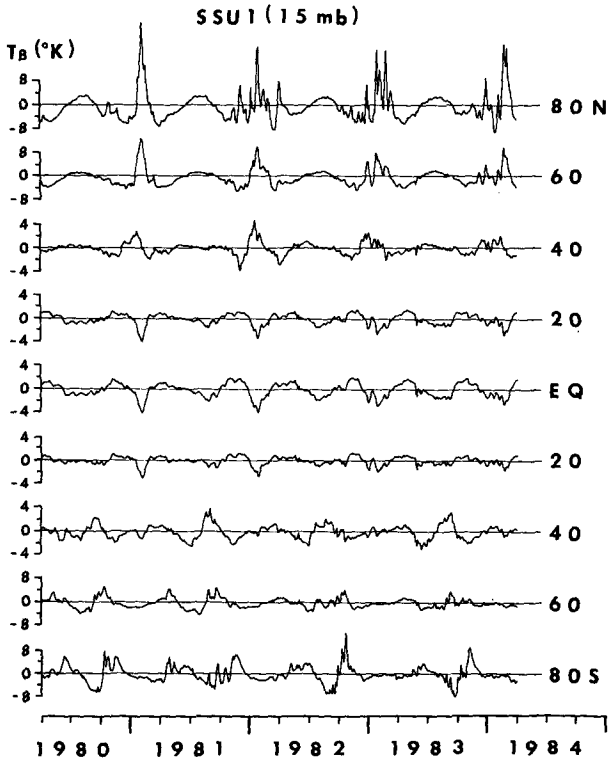

FIG. 4c. As in Fig. 4a but for SSU1 (15 mb).

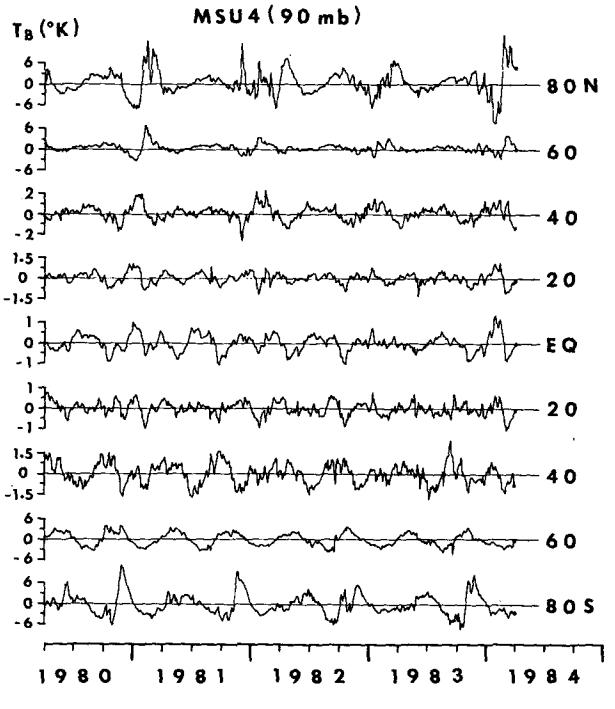

FIG. 4d. As in Fig. 4a but for MSU4 (90 mb).

f. A mechanism contributing to global SAO

In Fig. 4a–d we present four-year temperature time series for each of the stratospheric layers studied here. To allow short pulses to be more clearly seen, the series have been reconstructed from the Fourier coefficients with periods longer than six months removed. Major warming pulses in the NH winters can be traced well into the SH, but with reversal of phase: high latitude warming is strongly correlated with low latitude cooling. That such behavior exists for sudden stratospheric warming pulses has long been known (Fritz and Soules, 1970, 1972; Labitzke and Barnett, 1973); that similar behavior exists in the SAO temperature field (Fig. 2 and Table 1, and also seen in preliminary results presented in van Loon et al., 1972, Fig. 6) suggests the existence of a global-scale, meridional circulation on the SAO time scale.

To further test the idea that polar warming pulses can account for SAO features, individual winter and summer seasons in each hemisphere were separately analyzed for SAO. The results, given in Table 2, reveal that the strongest SAO occur near the NH pole and in NH winters. This, together with the well-known fact that major stratospheric polar warmings occur in the NH but not generally in the SH, suggests a close connection between polar stratospheric warmings and SAO. Intuitively, the superposition of such wintertime pulses on the annual temperature curve, with summertime solar heating, must contain significant Fourier amplitude at the SAO period. Furthermore, this six-month forcing would be expected to maximize near the latitudes where the winter warming pulses maximize, viz., the NH polar region; this is in fact where the analyses reveal the strongest SAO signal (Fig. 1 and Table 2).

The above argument would suggest that the dynamically induced stratospheric polar warmings provide an essential mechanism able to account, at least qualitatively, for these observed characteristics of the global SAO signal: (i) the polar and tropical maxima in temperature SAO, (ii) their anticorrelation, (iii) the mid-latitude minima in temperature SAO, (iv) the stronger polar SAO in the NH winter, compared with that in the SH winter, and (v) the large discrepancy in the NH winter between observed equatorial temperatures and calculations based on solar radiation (Fritz, 1974).

Acknowledgment. Support for this work has been provided by the National Science Foundation and the National Aeronautics and Space Administration through grants ATM8402901 and ATM8603943. We appreciate the diligent work of two reviewers whose comments significantly enhanced the organization and clarity of the presentation.

REFERENCES

Angell, J. K., and J. Korshover, 1970: Quasi-biennial, annual, and semiannual zonal wind and temperature harmonic amplitudes and phases in the stratosphere and low mesosphere of the Northern hemisphere. *J. Geophys. Res.*, **75,** 543–550.

Barnett, J. J., 1974: The mean meridional temperature behavior of the stratosphere from November 1970 to November 1971 derived from measurements by the Selective Chopper Radiometer on Nimbus IV. *Quart. J. Roy. Meteor. Soc.*, **100,** 505–530.

Crane, A. J., 1979: Annual and semiannual waves in the temperature of the mesosphere as deduced from Nimbus 6 PMR measurements. *Quart. J. Roy. Meteor. Soc.*, **105,** 509–520.

Fritz, S., 1974: On the causes of the annual and semiannual variation of radiance (or temperature) from the tropical stratosphere. *J. Atmos. Sci.*, **31,** 813–822.

——, and S. D. Soules, 1970: Large-scale temperature changes in the stratosphere observed from Nimbus III. *J. Atmos. Sci.*, **27,** 1091–1097.

——, and ——, 1972: Planetary variations of stratospheric temperatures. *Mon. Wea. Rev.*, **100,** 582–589.

Gao, X.-H., and J. L. Stanford, 1986: Low-frequency oscillations of the large-scale stratospheric temperature field. *J. Atmos. Sci.*, **44** (1987, in press).

Hamilton, K., 1986: Dynamics of the stratospheric semiannual oscillation. *J. Meteor. Soc. Japan,* **64,** 227–244.

Hayashi, Y., 1982: Space–time spectral analysis and its applications to atmospheric waves. *J. Meteor. Soc. Japan,* **60,** 156–171.

Hirota, I., 1980: Observational evidence of the semiannual oscillation in the middle atmosphere—A review. *Pure Appl. Geophys.* **118,** 217–238.

Hitchman, M. H., and C. B. Leovy, 1986: Evolution of the zonal mean state in the equational middle atmosphere during October 1978–May 1979. *J. Atmos. Sci.*, **43,** 3159–3176.

Holton, J. R., and W. M. Wehrbein, 1980: A numerical model of the zonal mean circulation of the middle atmosphere. *Pure Appl. Geophys.*, **118,** 284–306.

Labitzke, K., and J. J. Barnett, 1973: Global time and space changes of satellite radiances received from the stratosphere and lower mesosphere. *J. Geophys. Res.*, **78,** 483–496.

McGregor, J., and W. A. Charpman, 1978: Observations of the annual and semiannual wave in the stratosphere using Nimbus 5 SCR data. *J. Atmos. Terres. Phys.*, **40,** 677–684.

Meyer, W. D., 1970: A diagnostic numerical study of the semiannual variation of the zonal wind in the tropical stratosphere and mesosphere. *J. Atmos. Sci.*, **27,** 820–830.

Nastrom, G. D., and A. D. Belmont, 1975: Periodic variations in stratospheric-mesospheric temperature from 20–65 km at 80 N to 30 S. *J. Atmos. Sci.*, **32,** 1715–1722.

Reed, R. J., 1962: Some features of the annual temperature regime in the tropical stratosphere. *Mon. Wea. Rev.*, **90,** 211–215.

Takahashi, M., 1984: A two-dimensional numerical model of the semiannual zonal wind oscillation. *J. Meteor. Soc. Japan.*, **62,** 52–67.

van Loon, H., K. Labitzke and R. L. Jenne, 1972: Half-yearly wave in the stratosphere. *J. Geophys. Res.*, **77,** 3846–3855.

Yu, W.-B., R. L. Martin and J. L. Stanford, 1983: Long and medium-scale waves in the lower stratosphere from satellite-derived microwave measurements. *J. Geophys. Res.*, **88,** 8505–8511.